Advanced Steel Construction – Vol. 19 No. 1 (2023) 1–8
DOI:10.18057/IJASC.2023.19.1.1
(**Special Issue:** *10th International Conference on Advances in Steel Structures, ICASS'2020, Chengdu, China*)

COLLAPSE RESISTANCE CALCULATION WITH DIFFERENT STIFFNESS CONNECTIONS BASED ON THE COMPONENT METHOD

Zheng Tan [1], Wei-Hui Zhong [1, 2, *], Shi-Chao Duan [1], Chao-Fan Li [1], Yu-Hui Zheng [1] and Bao Meng [1]

[1] *School of Civil Engineering, Xi'an University of Architecture and Technology, Xi'an 710055, China*
[2] *Key Laboratory of Structural Engineering and Earthquake Resistance, Ministry of Education, Xi'an University of Architecture and Technology, Xi'an 710055, China*
** (Corresponding author: E-mail: zhongweihui1980@163.com)*

ABSTRACT

The collapse performance of steel frames generally depends on their ability to resist local damage. However, this ability is decided by the connection behavior, which has not been determined methodically and reliably. Thus, developing a simplified connection model for predicting the structural collapse resistance is critical for preventing progressive collapse. In this study, component models were constructed with different stiffness connections, including the double web angle (DWA), top-seat with double web angle (TSDWA), and welded flange-bolted web (WUF) connections, according to the component method by simplifying its geometry and dividing it into several basic springs. The proposed component-based connection models with detailed components were implemented within the finite element program, ANSYS. The models were validated against previous experimental tests. The analysis results indicate that the component models can accurately reflect the load response and post-fracture path of the assemblies with a cost-effective solution. This indicates that the component method is significant for progressive collapse analysis, providing a simple and effective tool for designers and engineers to evaluate the load-resisting capacities of steel frame structures.

ARTICLE HISTORY

Received: 20 July 2022
Revised: 22 August 2022
Accepted: 10 January 2023

KEYWORDS

Steel frame;
Different stiffness connections;
Progressive collapse;
Component method;
Numerical simulation

1. Introduction

In recent years, structural progressive collapse has become a topic of considerable research interest in the field of the civil engineering [1–2]. Preventing progressive collapse is a necessary task in structural engineering theory and practice. Progressive collapse primarily results from a chain reaction caused by local damage spreading to other structural components owing to overloading or accidental loads.

Connection failure primarily triggers structural failure and determines whether the internal force can be transmitted effectively. Many experimental studies and numerical analyses have showed that the connection behavior determines the mechanism resistances of frame structures, including compressive arch action, flexural action, and catenary action [3-4]. Therefore, beam–to–column connections are critical components in the anti-collapse design of steel frame structures. Accordingly, it is urgent to develop a simplified connection component model for predicting the mechanical behavior of beam–to–column connections. The most used modeling methods for the numerical simulation analysis of the frame structure collapse resistance include micro (refined modeling) [5–9], macro (node models based on beam or shell elements and component methods) [10], and multiscale hybrid (mixed elements of various types) [11–12] modeling methods. The results obtained by the refined modeling method are the most accurate; however, a systematic parameter analysis using the refined modeling method typically results in high modeling costs and long calculation time, particularly for full-size multistory frame structures. A reasonable component model can significantly increase computational efficiency of the numerical model when replacing the refined model for the structure design and collapse analysis.

With respect to the simplified modeling of steel structures, to investigate the relative performance of the beam–to–column connection, Sarraj et al. [13] and Liu et al. [14] performed component modeling. Yang et al. [15] tested seven different connections under failure condition of middle column through a static loading test. They found that the axial force and rotation of beam end determine the failure mode of the connections. Tan et al. [16] studied the performance of a beam–column assembly with different stiffnesses via static loading tests and demonstrated that different types of connections significantly influence the collapse resistance. Beam–to–column connections are typically subjected to combined tension, bending, and shear forces during the progressive collapse process.

In this study, numerical models of the beam–column assemblies were constructed with different stiffness connections, including the double web angle connection (DWA), top-seat with double web angle connection (TSDWA), and welded flange-bolted web connection (WUF), according to the component method proposed by Eurocode 3 (EC3) [17] by simplifying the geometrical composition of the connections. Subsequently, the applicability and efficiency of these simplified models were validated against previous experimental results.

2. Construction of the component models with different stiffness con nections

2.1. Simplified component method modeling

A connection can be simplified into a series of independent fundamental components using the component method (each fundamental component may consist of several mechanical springs). The overall mechanical properties of the connections can be analyzed by studying the nonlinear mechanical characteristics of each component of the connections. Accordingly, the overall response of the connections can be obtained through the collection of components. Applying the component method is significant for analyzing the working mechanism of each connection part. In addition, it can rapidly analyze and accurately acquire the mechanical properties of the beam–column assembly.

2.2. Mechanical behavior analysis of each spring (component)

Determining the mechanical properties of a connection by directly analyzing the deformation mechanism is challenging. The European code EC3 [17] proposes that the connections can be discretized into multiple mechanical units contributing to the force. The components (springs) were integrated to simulate the force state of the connections accurately, with appropriate assumptions. Accordingly, the DWA, TSDWA, and WUF connections comprised the following individual spring forces: connecting plate bolt hole compression (S1), bolt shear (S2), beam web bolt hole compression (S3), bolt tension (S4), angle bending (S5), and beam flange tension–compression (S6) springs. The DWA connection comprised the bolt hole compression spring at the connecting plate, compression spring at the beam web, and bolt shear spring. The TSDWA connection comprised the following individual spring forces: bolt hole compression spring at the angle, bolt shear spring, bolt hole compression spring at the beam, and bolt tension and angle bending springs. The WUF connection comprised the connecting plate compression, beam web compression, bolt shear, and beam flange tension–compression spring forces. These springs can be simplified further according to their serial and parallel relationships. Different springs were combined to form an equivalent component in series to model the different connections, as shown in Fig. 1.

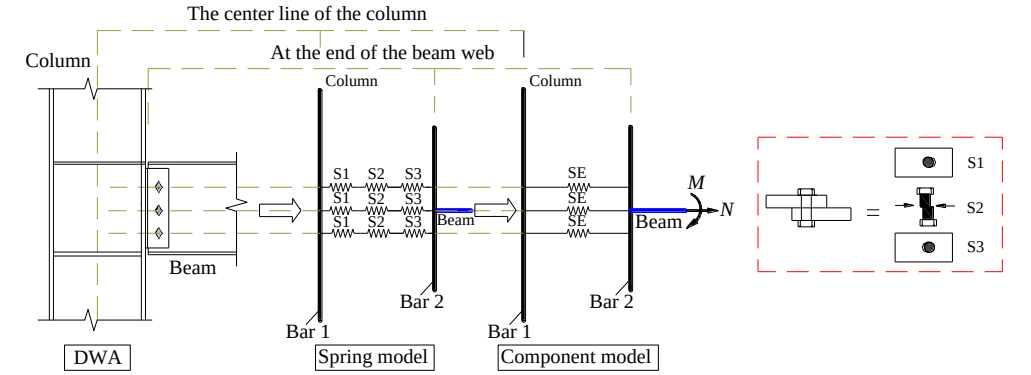

(a) DWA connection

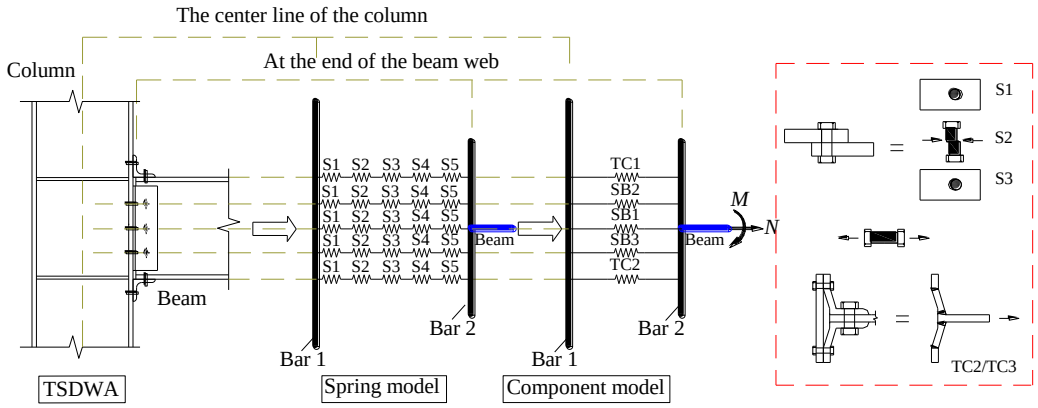

(b) TSDWA connection

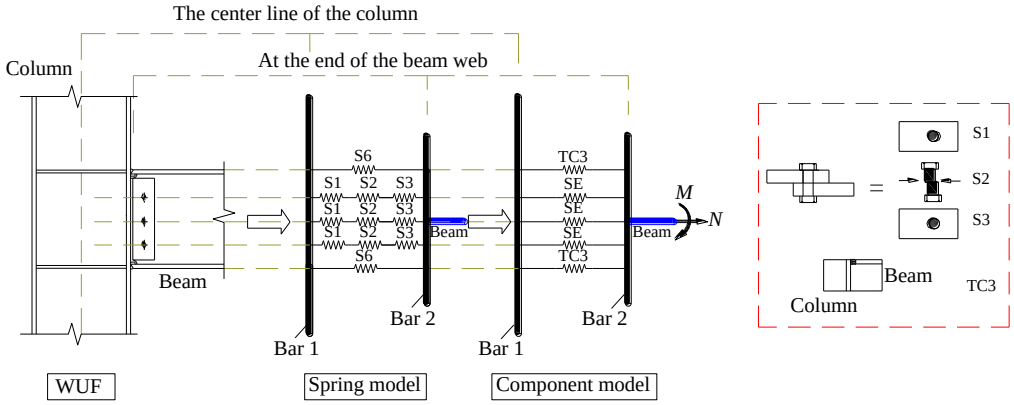

(c) WUF connection

Fig. 1 Component model of different stiffness connections

2.2.1. Bolt hole compression spring (S1/S3)

The S1 and S3 springs correspond to the deformation of the bolt holes of the connecting plate and beam web, respectively, as illustrated in Fig. 2. Deformation was significantly affected by the end and edge distances of the bolt holes.

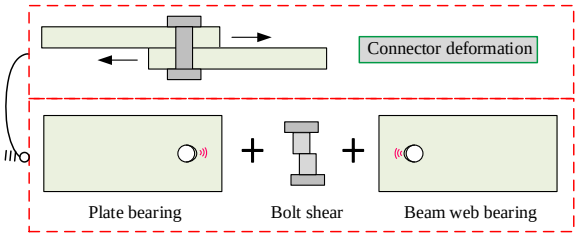

Fig. 2 Deformation decomposition of a single component

Elsalti and Richard [18] proposed the following equations to define the relationship between the load and deformation of a bolt hole compression spring:

$$\frac{F}{F_{b,Rd}} = \frac{1.74\Lambda}{(1+\Lambda^{0.5})^2} - 0.009\Lambda \tag{1}$$

$$\Lambda = \Delta\beta k_i F_{b,Rd} \tag{2}$$

where F is the load applied to the bolt hole (plate), F_{bRd} is the ultimate bearing capacity of the bolt hole (plate), Λ is the nominal pressure deformation of the bolt hole, Δ is the pressure deformation of the bolt hole, and β is the material correction factor (steel is typically 1.0).

Fisher and Struik [19] derived the ultimate bearing capacity formula with considering the bolt hole shear failure mode:

$$F_{T,Rd} = \frac{e_2}{d_h} \times f_u \times d_h \times t \le 2.4 f_u dt \tag{3}$$

where e_2 is the distance between the bolt holes (the distance between the center of the bolt hole and the edge of the plate along the direction of the

main force), d_h is the diameter of the bolt hole, f_u is the tensile strength, and t and d are the thickness and width of the plate, respectively.

The deformation of the bolt hole consists of three parts [18]: extrusion of the bolt hole (corresponding stiffness k_{br}), bending deformation of the steel plate at the outer end of the bolt hole (corresponding stiffness k_b), and shear deformation of the steel plate at the outer end of the bolt hole (corresponding stiffness k_v), as shown in Fig. 3. Each stiffness can be calculated using the following formula [20]:

$$k_{br} = 120 t f_y (d_b / 25.4)^{0.8} \tag{4}$$

$$k_b = 32 E t (e_2 / d_b - 1/2)^3 \tag{5}$$

$$k_v = 6.67 G t (e_2 / d_b - 1/2) \tag{6}$$

where f_y, E, and G are the yield strength, modulus of elasticity, and shear modulus, respectively, and d_b is the bolt shank diameter.

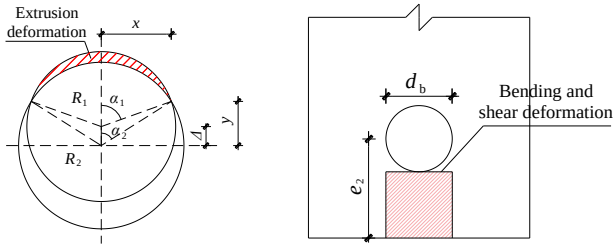

(a) Extrusion deformation of bolt hole (b) Bending and shear deformation of bolt hole

Fig. 3 Deformation of the bolt hole

Thus, the bolt hole compression stiffness k_i can be represented by the following equation:

$$k_i = \frac{1}{\frac{1}{k_{br}} + \frac{1}{k_b} + \frac{1}{k_v}} \tag{7}$$

Fig. 4 shows the load–deformation (F–Δ) curve of the bearing deformation spring of the bolt hole (only the plate thickness was different for the connecting plate, angle, beam flange, and beam web) [13].

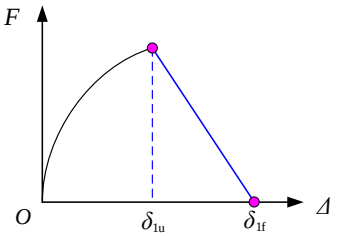

Fig. 4 Load–deformation curve of bearing deformation spring of a bolt hole

2.2.2. Bolt shear spring (S2)

The relationship between the shear force and shear deformation curve of the S2 spring can be determined using the modified Raberg–Osgood formula [21]:

$$v_{v,b} = \frac{F_v}{k_{v,b}} + \Omega \left(\frac{F_v}{F_{v,Rb}}\right)^6 \tag{8}$$

where $v_{v,b}$ and F_v are the shear deformation and shear force of the bolts, respectively, $k_{v,b}$ is the shear stiffness of the bolts, Ω is a coefficient related to the temperature and remains to be 2.5 at normal temperature, and the ultimate shear strength of the bolts is

$$F_{v,Rb} = 0.6 \times F_{u,b} \times A_b \tag{9}$$

where $f_{u,b}$ is the ultimate tensile strength of the bolts and, A_b is the effective area of the bolt shank.

The shear stiffness of bolts can be obtained as follows:

$$k_{v,b} = \frac{kGA}{d_b} \tag{10}$$

where k is the correction coefficient for bolt shear deformation, equal to 0.15 [22].

2.2.3. Bolt tension spring (S4)

The load–deformation curve of S4 can be determined by the simple tensile deformation method according to the effective area and material properties of the bolt and can be simplified to a bilinear strength relationship model.

2.2.4. Angle bending spring (S5)

The load–deformation curve of S5 can be simplified into three stages [23] according to EC3 [17], as shown in Fig. 5.

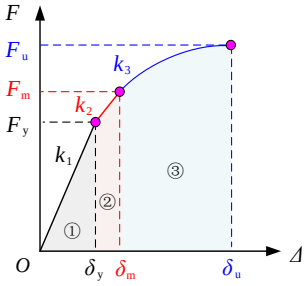

Fig. 5 Load–deformation curve of bearing deformation spring of a bolt hole

The values of F_y and F_m can be determined using the following formulas [24]:

$$F_y = \frac{2}{3} F_{T,Rd} \tag{11}$$

$$F_m = F_{T,Rd} \tag{12}$$

where $F_{T,Rd}$ is the yield-bearing capacity of angle steel connectors.

The initial stiffness k_1 [23] of angles in bending is

$$k_1 = \frac{0.5 E b_{eff,a} t_a^3}{(m - t_a - 0.8 r_a)3} \left(\frac{4\gamma_a}{\gamma_a + 3}\right) \tag{13}$$

$$\gamma_a = \frac{I_2 / L_2}{I_1 / L_1} \tag{14}$$

where I_1, I_2, L_1, and L_2 are defined in Fig. 6, $b_{eff,a}$ is the effective effect width of the bolted angles, $b_{eff,a}$ can be calculated using Table 1 (Fig. 7 shows the dimension parameters of the connection), t_a is the thickness of the angles, the value of m and r_a are defined in Fig. 7.

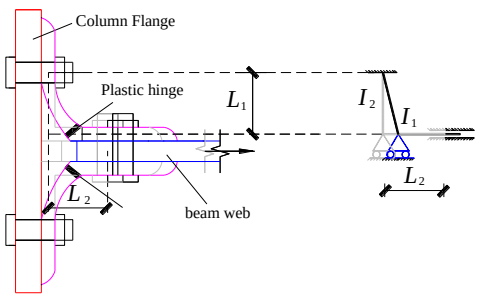

Fig. 6 Mechanical bending model of angle component

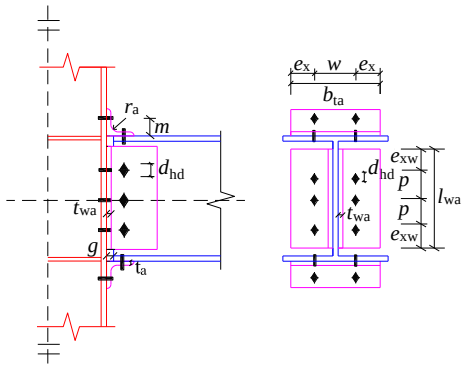

Fig. 7 Dimension parameters of the connection

Table 1
Effective width of angle components [25]

Bolt row	Effective width
Top angle, Bottom angle	$b_{efft,ta}$ = min(d_h+2m_a, d_h/2+m_a+w/2; b_{ta}/2; e_x+d_h/2+m_a)
Inner bolt row web angle	$b_{efft,ta}$ = min(d_h+2m_a, p)
End bolt row of web angle	$b_{efft,ta}$ = min(d_h+2m_a, d_h/2+m_a+p/2; e_x+p/2; e_{xw}+d_h/2+m_a)

k_2 is the stiffness of the transitional period, which was set as 1/7k_1 [22] until it reached the yield capacity of the angles. For the convenience of analysis, the component of the bending angles can be considered as an equivalent bolted T-stub, and the design resistance of the T-stub can be calculated as the smallest value among the three possible failure modes, as illustrated in Fig. 8.

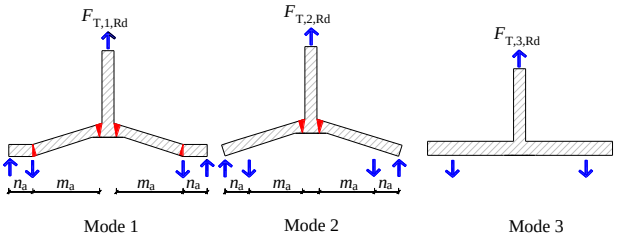

Fig. 8 Three possible failure modes of T-stub component

Mode 1: A plastic hinge appeared near the bolt of the T-stub flange (complete yielding of the T-stub flange).

$$F_{T,1,Rd} = \frac{4M_a}{m_a} = \frac{b_{eff,a}t_a^2 f_y}{m_a} \tag{15}$$

Mode 2: A plastic hinge appeared near the bottom of the T-stub flange (bolt failure with yielding of the T-stub flange).

$$F_{T,2,Rd} = \frac{2M_a + n_a\sum B_{T,Rd}}{m_a + n_a} \tag{16}$$

Mode 3: The bolt rod reached its tensile design bearing capacity (bolt failure).

$$F_{T,3,Rd} = \sum B_{T,Rd} \tag{17}$$

where M_a is the plastic bearing capacity of the T-stub, $B_{T,Rd}$ is the bolt design resistance, and m_a and n_a are the distance between the two plastic hinges and the distance between the bolt center lines and prying force position, respectively, as shown in Fig. 8.

m_a can be calculated as follows [23]:

$$m_a = m_{a,EC3} - \psi_1\left(\frac{d_{bd}}{2} + \frac{t_a}{2} + 0.2r_a\right) \tag{18}$$

$$\psi_1 = 1.89 - \frac{3.22t_a}{d_b\sqrt{m_{a,EC3}/d_b}} \tag{19}$$

where ψ_1 is a coefficient in the range 0–1, and d_{bd} is the bolt head diameter. $m_{a,EC3}$ can be calculated as follows:

$$m_{a,EC3} = \begin{cases} m - t_a - 0.8r_a & g \le 0.4t_a \\ m - 0.5t_a & g > 0.4t_a \end{cases} \tag{20}$$

where g is the gap between the column flange and beam flange, as shown in Fig. 7.

Relevant tests show that when one of the aforementioned stress modes is formed, the angle steel connection will yield in bending, and its bearing capacity can be improved further. This indicates that the load–deformation curve will continue to rise in the later stage, causing the stiffness to decline and enter the large deformation stage. The incremental iteration method [24] can be employed to determine the bearing capacity according to the analysis model shown in Fig. 9 as follows:

$$\begin{aligned} \Delta F &= F_2 - F_1 = N_a(\sin\theta_2 - \sin\theta_1) \\ &= N_a\left(\frac{\delta_1 + \Delta}{\sqrt{m^2 + (\delta_1 + \Delta)^2}} - \frac{\delta_1}{\sqrt{m^2 + \delta_1^2}}\right) \end{aligned} \tag{21}$$

$$N_a = (b_{eff,a} - nd_b)t_a f_u \tag{22}$$

where n is the number of bolts.

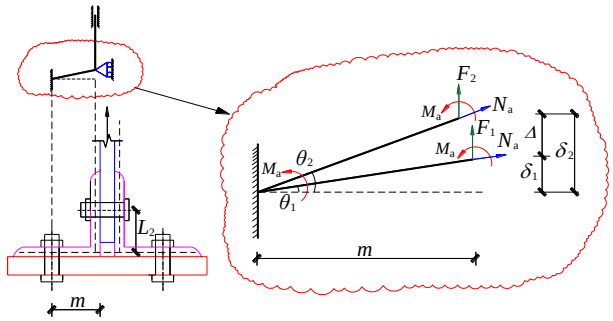

Fig. 9 Mechanical model of the angle at the large deformation stage

When mode 1 or 2 is formed, a plastic hinge appears in the component, and the ultimate displacement δ_u of spring S6 [25] can be refereed as follows:

$$\delta_u = m^*(1 + \varepsilon_u)\sin\left(\frac{\varepsilon_u m^*}{2t_a}\right) \tag{23}$$

where ε_u is the ultimate displacement and m^* is the distance between the two plastic hinges at the horizontal legs of the angles.

$$m^* = m - t_a - 0.8r_a + \eta d_b \tag{24}$$

where η is a coefficient, which can be calculated as follows:

$$\eta = \begin{cases} 1.1335 - 0.00242\dfrac{f_{y,b}A_b b_{eff,a}}{F_{T,Rd}} & \dfrac{f_{y,b}A_b b_{eff,a}}{F_{T,Rd}} \le 560 \\ -0.22 & \dfrac{f_{y,b}A_b b_{eff,a}}{F_{T,Rd}} > 560 \end{cases} \tag{25}$$

where $f_{y,b}$ is the yield strength of bolts.

When stress mode 3 is formed, the ultimate displacement of S6 can be calculated using Eq. (21), and the load–deformation curve of S4 can be determined.

2.2.5. Beam flange tension–compression spring (S6)

The beam flange tension–compression spring S6 (the component comprises a deformation spring) was used to simulate the tension and compression effects of the upper and lower flange ends; Fig. 10 shows its load–deformation curve [25] (a positive value represents tension, and a negative value represents compression). The stress state must be distinguished first before determining the ultimate bearing capacity of the tension and compression of spring S5. The ultimate state is the material yield under compression and fracture under tension (ignoring compression flange buckling).

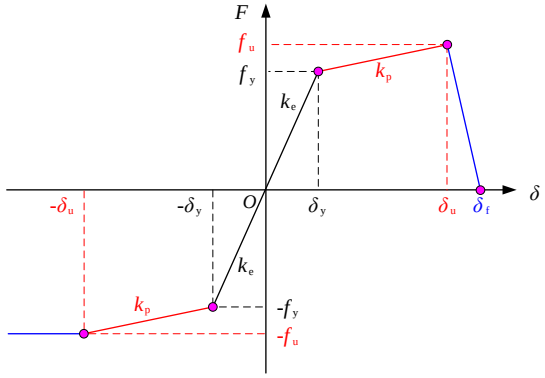

Fig. 10 Load–deformation curve of tension and compression spring at the beam flange

The relevant parameters of the TC component before yielding can be calculated as [25]

$$k_e = \frac{Eb_f t_f}{\rho b_s} \tag{26}$$

$$F_y = b_f t_f f_y \tag{27}$$

where k_e is the elastic stiffness of the flange tension compression component, b_f and t_f are the width and thickness of the beam flange, respectively, b_s is the width of the shear plate, and ρ is the coefficient [25] related to the failure modes (equal to 1.0 and 1.5 when the failure mode is controlled by the beam–to–column connection and beam flange, respectively).

The elastic–plastic stiffness at the strengthening stage can be calculated as

$$k_p = \frac{E_s k_e}{E} \tag{28}$$

where E_s is the strengthening modulus of the steel.

The ultimate bearing capacity of flange components in tension can be calculated as follows:

$$F_u = b_f t_f f_u \tag{29}$$

The load–deformation curves of the first two stages of the compression flange component were the same as those of the tension flange component. When the deformation reached δ_u, the load reached its limit and no longer increased in the final stage; however, the deformation continued to increase.

3. Component method application

3.1. Model verification tests

3.1.1. Specimens with DWA and TSDWA connections

Yang et al. [15] performed collapse tests with DWA and TSDWA connections; Fig. 11 presents the test setup and details of the two types of connections. The beam and column adopted standard sections of 256 mm × 146.4 mm × 6.3 mm × 10.9 mm and 215.8 mm × 206.4 mm × 10 mm × 17.3 mm, respectively. The sections of the top/seat and web angles were both L90 mm × 8 mm. The connections between beam ends and column flanges were realized by the steel angles and M20 Grade 8.8 bolts (the bolt hole diameter was 22 mm). The related material properties can be found in [15].

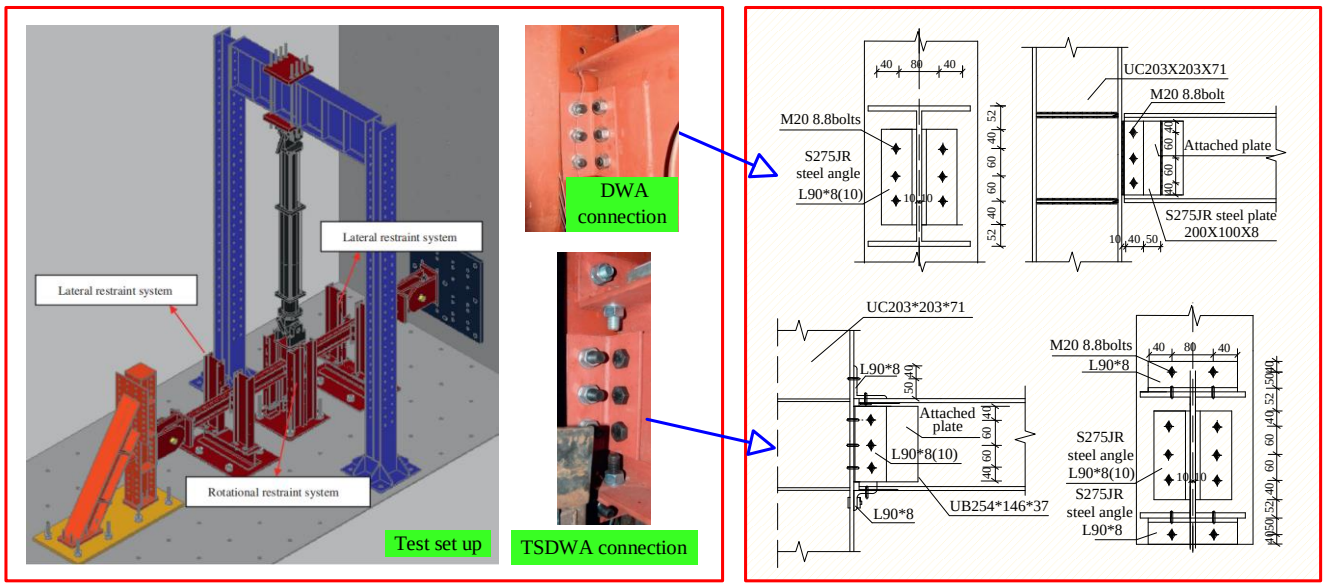

Fig. 11 Collapse tests of beam–column assemblies with DWA and TSDWA connections [15] (dimension units: mm)

Fig. 12 illustrates the final failure modes of the two specimens. During the actual test, the left and right sides of the middle column showed asymmetrical characteristics owing to the initial errors of steel and installation error of the specimens. Moreover, only three bolts on one side of the middle connection were broken in sequence during the entire loading process.

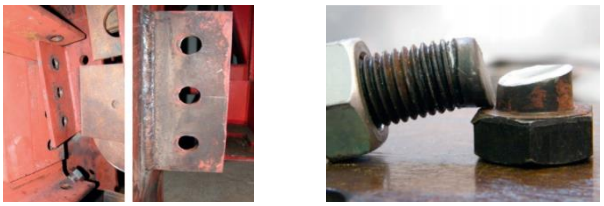

(a) DWA connection

(b) TSDWA connection

Fig. 12 Failure modes of the beam–column assemblies with DAW and TSDWA connections [15]

3.1.2. Specimen with WUF connection

A beam–column assembly with a WUF connection was tested in [26]; Fig. 13 shows the dimensions of the connections. The column and beam section dimensions were H539.5 mm × 210.69 mm × 11.56 mm × 18.8 mm and H481.84 mm × 286.13 mm × 16.64 mm × 26.92 mm, respectively. The dimensions of the connecting plate were 304.8 mm × 152.4 mm × 12.7 mm, and the diameter of the bolt was 25.4 mm (the bolt hole diameter was 27.4 mm). The material properties of all components are given in [26]. The bolt spacing was 101.6 mm, the edge distance between the bolt hole and beam web was 57.15 mm, and that between the bolt hole and connecting plate was 69.85 mm. Fig. 14 presents the final failure modes of the specimens with WUF connection.

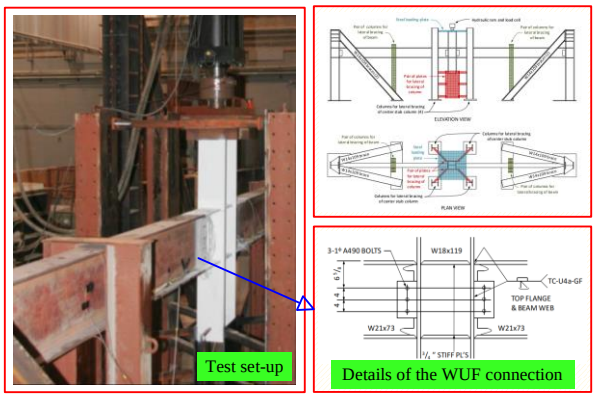

Fig. 13 Collapse tests of beam–column assemblies with WUF connection [26] (dimension units: in)

(a) Failure mode of the WUF connection

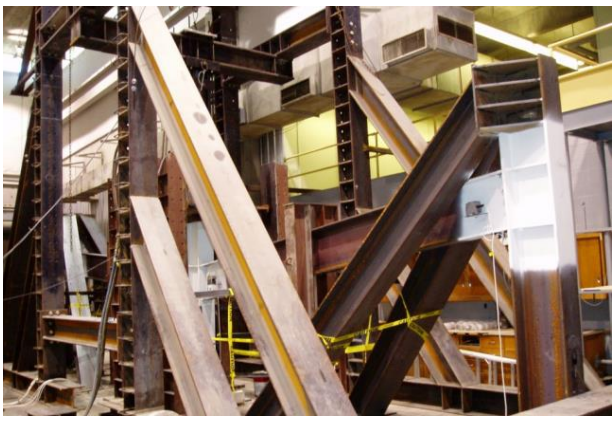

(b) Overall view of the specimen with WUF connection

Fig. 14 Final phenomenon of the specimen with WUF connection [26]

3.2. Load–deformation curves of equivalent components

Fig. 14 shows the load–deformation relationship of each component of the DWA, TSDWA, and WUF connections, calculated based on the discussion in Section 2.2.

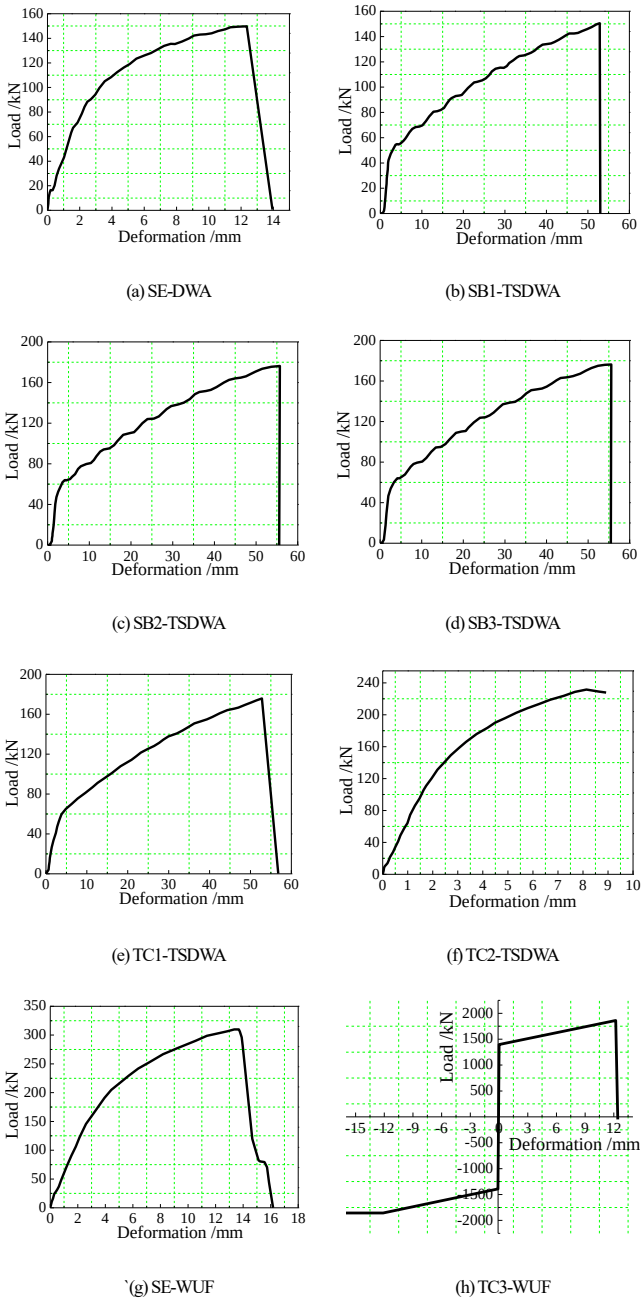

(a) SE-DWA (b) SB1-TSDWA

(c) SB2-TSDWA (d) SB3-TSDWA

(e) TC1-TSDWA (f) TC2-TSDWA

`(g) SE-WUF (h) TC3-WUF

Fig. 14 Component properties of different connections

3.3. Comparison of finite element modeling and test results by component method

In this study, numerical analysis models were established for the collapse resistant performance of single-story steel frames with different connections using LS-DYNA based on the geometrical dimensions and material properties of the specimens. The rigid rods in the beams, columns, and connection zone used the Hughes–Liu beam elements, and the MAT119 spring elements were used in each component. The beam–to–column connection domain was assumed to be a rigid zone consisting of four rigid rods. The end of the beam was provided with a rigid rod, and the two ends of the component were connected to the rigid rod and rigid zone, respectively. The upper and lower ends of the failure columns were connected to the rigid zone. The rigid rod and zone were coupled to realize the transmission of internal force. A vertical load under displacement-controlled was selected to the top of the failed column, and only vertical movement was allowed. The boundary conditions of the DWA and TSDWA were set to hinge connections, and the bottom of the side columns of

the WUF was fixed. The component models of steel frames with different connections are shown in Fig. 15. During the analysis and calculation, the constitutive relationship of each component was defined by the load–displacement curves in Fig. 14, while fracture occurs when a particular component unit fails during the loading process.

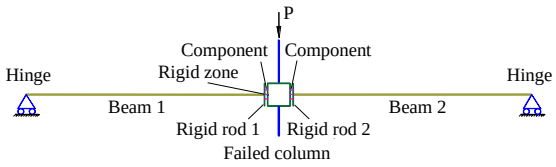

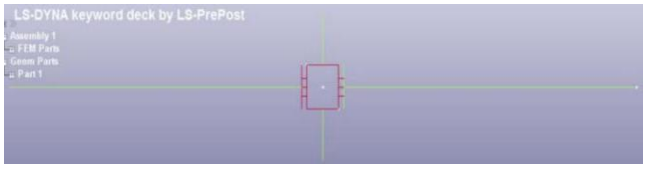

(a) DWA connection

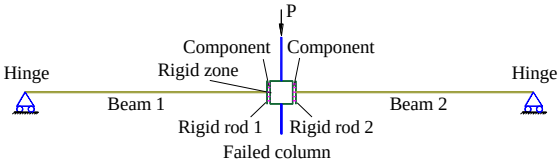

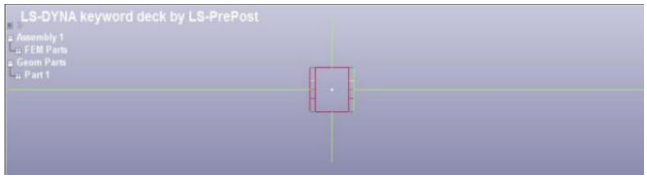

(b) TSDWA connection

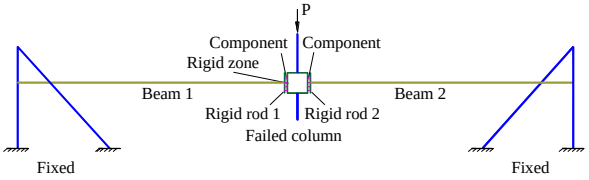

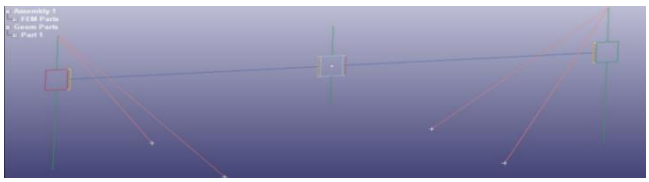

(c) WUF connection

Fig. 15 Component models of steel frames with different connections

According to the proposed component models with DWA, TSDWA, and WUF connections, the load–displacement curves and failure modes of the three specimens under an internal column removal scenario were obtained by numerical simulation are presented in Figs. 16 and 17. It can be observed that the results of the component model were consistent with the test results. Therefore, this method can reflect the primary progressive collapse responses of the beam–column assemblies with different stiffness connections. The fracture position and sequence can be simulated accurately, providing important reference for research on the resistance evaluation of steel frames with connections of different stiffnesses.

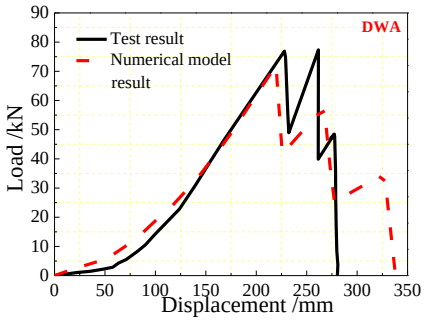

(a) DWA connection

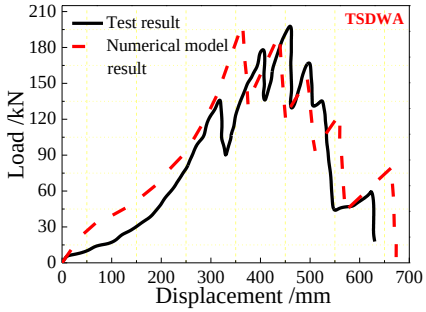

(b) TSDWA connection

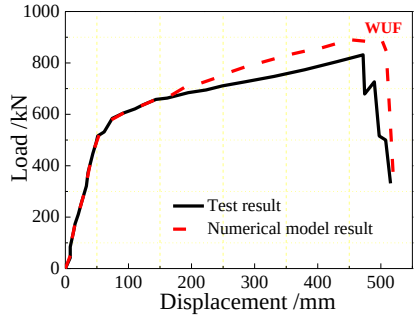

(c) WUF connection

Fig. 16 Comparison of load–displacement curves between tests and numerical models

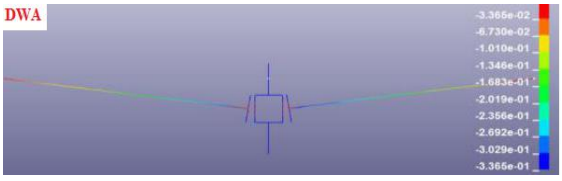

(a) DWA connection

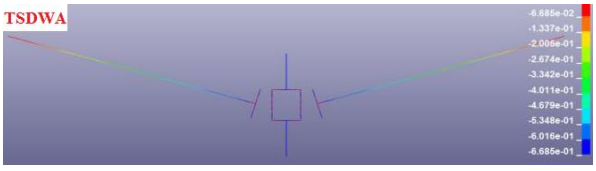

(b) TSDWA connection

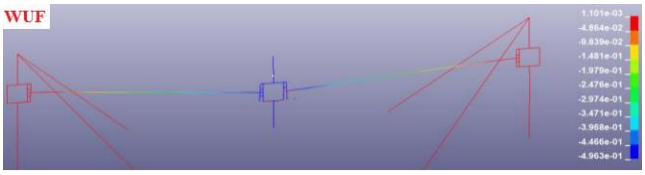

(c) WUF connection

Fig. 17 Final deformation of models with different connections predicted by the component models

4. Conclusion

(1) The connections of the steel structure with different stiffnesses can be divided into a series of independent basic mechanical springs according to their bearing mechanisms: bolt hole compression (S1/S3), bolt shear (S2), bolt tension (S4), angle bending (S5), and beam flange tension–compression (S6) springs.

(2) By analyzing the mechanical properties of each fundamental component comprising the beam–to–column connections, the accurate load–displacement curve of a single component can be obtained. Accordingly, the overall component analysis model of the connections can be constructed. This model can be employed to investigate further the overall mechanical characteristics of the connections of structures.

(3) A numerical analysis model for the collapse behavior of the beam–column assemblies with different stiffness connections was established based on the parameters of each fundamental component derived from the calculation examples. Behaviors, such as the load–displacement responses and failure modes, were consistent with the test results, satisfying the accuracy requirements of engineering calculations.

(4) Simplified component models with different connections based on the component method are highly accurate and efficient. The test results indicate that the proposed methods can predict structural resistance and progressive collapse performance, which was beneficial for research on structural anti-progressive collapse.

Acknowledgments

This research was supported by the National Natural Science Foundation of China [grant numbers 51678476, 51908449] and the Scientific Research Plan Projects of the Shaanxi Education Department [grant numbers 20JY033, 20JK0713]. All opinions, findings, conclusions, and recommendations expressed in this paper are those of the authors and do not necessarily reflect the views of the sponsors.

References

[1] Meng B., Li L.D., Zhong W.H., et al., “Improving anti-progressive collapse capacity of welded connection based on energy dissipation cover-plates”, Journal of Constructional Steel Research, 188, 107051, 2022.

[2] Meng B., Hao J.P. and, Zhong W.H., “Numerical study on the anti-progressive collapse performance of steel frame-steel plate shear wall structures”, Journal of Building Engineering, 35, 102049, 2021.

[3] Tan Z., Zhong W.H., Meng B., et al., “Effects of the numbers of stories and spans on the collapse-resistance performance of multi-story steel frame structures with reduced beam section connections”, Advanced Steel Construction, 18(2), 616-628, 2022.

[4] Zhong W.H., Tan Z., Song X.Y., et al., “Anti-collapse analysis of unequal span steel beam–column substructure considering the composite effect of floor slabs”, Advanced Steel Construction, 15(4), 377–385, 2019.

[5] Ahmadi E. and Hosseini S.A., “Capacity evaluation of eight bolt extended endplate moment connections subjected to column removal scenario”, Advanced Steel Construction, 17(3), 273–282, 2021.

[6] Zhong W.H., Tan Z., Tian L.M., et al., “Collapse resistance of composite beam-column assemblies with unequal spans under an internal column-removal scenario”, Engineering Structures, 206, 110143, 2020.

[7] Tan Z., Zhong W.H., Meng B., et al., “Numerical evaluation on collapse-resistant performance of steel-braced concentric frames ”, Journal of Constructional Steel Research, 193, 107268, 2022.

[8] Li G.Q., Zhang J.Z. and Jiang J., “Multi-story composite framed-structures due to edge-column loss”, Advanced Steel Construction, 16(1), 20–29, 2020.

[9] Tan Z., Zhong W.H., Tian L.M., et al., “Quantitative assessment of resistant contributions of two-bay beams with unequal spans”, Engineering Structures, 242, 112445, 2021.

[10] Adam J.M., Parisi F., Sagaseta J., et al., “Research and practice on progressive collapse and robustness of building structures in the 21st century”, Engineering Structures, 173, 122–149, 2017.

[11] Tan Z., Zhong W.H., Tian L.M., et al., “Numerical study on collapse-resistant performance of multi-story composite frames under a column removal scenario”, Journal of building Engineering, 44, 102957, 2021.

[12] Zheng L. and Wang W.D., “Multi-scale numerical simulation analysis of CFST column-composite beam frame under a column-loss scenario”, Journal of Constructional Steel Research, 190, 107151, 2022.

[13] Sarraj M., “The behavior of steel fin plate connections in fire”, Sheffield : University of Sheffield, 2007.

[14] Liu C., Tan K.H. and Fung T.C., “Component-based steel beam–column connections modelling for dynamic progressive collapse analysis”, Journal of Constructional Steel Research, 107(1), 24-36, 2015.

[15] Yang B. and Tan K.H., “Experimental tests of different types of bolted steel beam-column joints under a central-column-removal scenario”, Engineering Structures, 54, 1112-1130, 2013.

[16] Tan Z., Zhong W.H., Tian L.M., et al., “Research on the collapse-resistant performance of composite beam-column substructures using multi-scale models”, Structures , 27, 86–101, 2020.

[17] EN1993-1-8. Eurocode 3: Design of Steel Structure, Part 1-8: Design of joints. Brussels: European Committee for standardization; 2005.

[18] Elsalti M.K. and Richard R.M., “Derived moment rotation curves for partially restrained connections”, Development in Structural Engineering Computing, 18: 55-62, 2009.

[19] Fisher J.W, and Struik J.K., “Guide to design criteria for bolted and riveted joints”, New York: Wiley Interscience Press, 1974.

[20] Rex C.O, and Easterling S.W., “Behavior and modeling of a bolt bearing on a single plate”, Journal of Structural Engineering, 129(6), 792-88, 2003.

[21] Ramberg W. and Osgood W.R., “Description of stress–strain curves by three parameters”, Washington DC: National Advisory Committee for Aeronautics, 1943.

[22] Hayes M.D., “Structural analysis of a pultruded composite beam: shear stiffness determination and strength and fatigue life predictions”, Blacksburg: Faculty of the Virginia Polytechnic Institute and State University, 2003.

[23] Faella C., Piluso V. and Rizzano G., “Structural steel semirigid connections: theory, design and software”, Florida: Chemical Rubber Company Press, 2000.

[24] Yang B. and Tan K.H., “Robustness of bolted-angle connections against progressive collapse: mechanical modeling of bolted-angle connections under tension”, Engineering Structures, 547(12), 153-168, 2013.

[25] Yim H.C, and Krauthammer T., “Mathematic-mechanical model of WUF-B connection under monotonic load”, Engineering Journal, 2(1), 71-90, 2010.

[26] Sadek F., Main J.A., and Lew H.S., “An experimental and computational study of steel moment connection under a column removal scenario”, Gaithersburg: National Institute of Standards and Technology, 2010.